



standard photolithographic techniques and actuated with PPy(DBS)-gold bilayer as hinges.<sup>7</sup>

However, in order for these materials to be used as conventional actuators, it is important to accurately characterize their electromechanical properties. In particular, it is necessary to quantify the electrochemically induced surface stress (which leads to the bending of the bilayer) so that mechanical limitations, repeatability, durability, and potential advantages of this system can be determined.<sup>8</sup> Micromechanical cantilever-based sensors, with their high sensitivity and fast response times, are ideal tools for the characterization of these molecular scale electromechanical actuators.<sup>9,10</sup> Such micromechanical devices, based on commercially available atomic force microscopy (AFM) microcantilevers, have the potential to transduce a variety of chemical and physical phenomena into a mechanical movement on the nanometer scale.<sup>11,12</sup>

In this article, we present surface stress results for dodecyl benzenesulfonate-doped polypyrrole (PPy(DBS)) films actuated by cyclic voltammetry in aqueous solutions. The bending response of the PPy(DBS)/Au-coated silicon microcantilever is measured as a function of the applied potential, simultaneously yielding real-time, in situ, electrochemical, and surface stress information. We discuss the surface stress sensor's response during the anomalous first reductive scan as well as the effect of long-term cycling on the mechanical transformation ability of PPy(DBS) actuators in both surfactant (NaDBS) and halide- (NaCl) based electrolyte.

## 2. Experimental Section

**2.1. Materials and Methods.** All experiments were performed in the cell described below. Prior to each experiment, the cell is rinsed three times with deionized water (Millipore Simplicity 185 water system), followed by the electrolyte solution. The pyrrole monomer liquid (98%, Aldrich, Canada) is purified by passage through an alumina-filled column. The resulting liquid is clear and colorless in appearance, indicating that long pyrrole chains, from adventitious polymerization, are removed. The aqueous solution containing pyrrole and NaDBS (98%, Aldrich, Canada) is protected from ambient light following its preparation to prevent polymerization of the monomer. All other electrolyte solutions (except for the surfactant-based, which produces some foam) are purged for 1 h with argon gas to remove oxygen contamination from the solution before use. During experiments, a small positive pressure of argon is kept above the electrochemical cell.

The microcantilever sensors used herein are rectangular silicon cantilevers from MikroMasch (Estonia) type CSC12/without Al/tipless, with a typical length, width, thickness, and spring constant of 350  $\mu\text{m}$ , 35  $\mu\text{m}$ , 1  $\mu\text{m}$ , and 0.03 N/m, respectively. However, these dimensions and spring constant were independently measured for each microcantilever used in order to improve on the accuracy of the measured surface stress.

**2.2. The Instrument.** An instrument was constructed to integrate an AFM microcantilever-based sensor with a standard three-probe electrochemical system, the details of which are described elsewhere.<sup>13</sup> In short, the electrochemical setup uses an Ag/AgCl reference electrode, RE, (model RE-6, BioAnalytical Systems, USA), and a platinum wire as a counterelectrode, CE, (99.99% purity, Alpha Aesar, USA). These are both inserted in the top of a Teflon cell. A gold-coated, rectangular-shaped silicon microcantilever serves as both the working electrode (WE) and as the sensing platform of the surface stress sensor. A commercial potentiostat (model 50CW, BioAnalytical Systems, USA) is used to apply a potential to the microcantilever

(WE) and to monitor the current response during cyclic voltammetric experiments. In parallel, an optical beam technique<sup>13,14</sup> is used to monitor the microcantilever deflection for the surface stress measurements. The laser light is focused on the silicon backside of the microcantilever to avoid artifacts in the deflection measurement resulting from changes in reflectivity of the conducting polymer film.

To perform electrochemical experiments on the surface of a silicon microcantilever, one of its sides was rendered electrically conductive by thermally evaporating a 100-nm film of Au (99.99%, Plasma Materials, USA) on a 10-nm Ti (99.99%, Alfa Aesar, USA) adhesion layer. The evaporation was conducted at a pressure below  $5.0 \times 10^{-6}$  Torr at a rate of 0.14 nm/s for Au, and 0.04 nm/s for Ti. Radiative heating of the evaporation boat increased the microcantilevers' temperature to  $130 \pm 20$  °C. The resulting Au film has an average grain size of  $100 \pm 60$  nm with a RMS roughness of  $1.0 \pm 0.2$  nm, on a 1- $\mu\text{m}$  length scale as determined by AFM.

To avoid the possibilities of electrochemical reactions occurring at the contact point, the microcantilever (WE) is vertically immersed into the electrolyte with a micropositioner so that only the microcantilever and a small portion of the chip (onto which the cantilever beam is clamped on) are in the solution.

**2.3. Surface Stress.** The optical beam deflection technique used in this instrument measures the deflection of the free end of a microcantilever,  $\Delta z$ . The surface stress ( $\Delta\sigma$ ) is in turn directly proportional to the microcantilever deflection ( $\Delta z$ ) through:<sup>15</sup>

$$\Delta\sigma = \frac{4}{3(1-\nu)} \cdot \frac{l}{wt} k_{\text{rect}} \Delta z \quad (2)$$

where  $\nu$ ,  $l$ ,  $w$ ,  $t$ , and  $k_{\text{rect}}$  are the Poisson's ratio, length, width, thickness, and spring constant of the microcantilever, respectively. The value of  $t$  is taken as the thickness of the microcantilever beam up to the Au-PPy film interface. Indeed, the surface stress responsible for the mechanical motion of the beam is generated at this interface. In addition, the elastic modulus of a PPy film is at least 2 orders of magnitude smaller than Si, so that changes of the film elastic properties during redox processes are negligible. By carefully determining the value of each parameter in eq 2, we can measure surface stress values with an accuracy of 10%.<sup>13</sup> By definition, a compressive (tensile) surface stress bends the microcantilever away from (toward) the stressed surface, and is assigned a negative (positive) sign. Thermodynamically, the surface stress is related to the surface free energy by the Shuttleworth equation. A recent communication by Lipkowski et al.<sup>16</sup> summarizes the current knowledge on thermodynamic of solid electrodes.

**2.4. Pretreatment of the WE Gold Surface.** The gold surface is electrochemically cleaned in 0.1 M HClO<sub>4</sub> solution, preceding the deposition of the conjugated polymer onto the gold-coated microcantilever. The voltage is swept from 0 to 1500 mV (all potentials quoted in this paper are versus Ag/AgCl) at a scan rate of 20 mV/s (Figure 2). This procedure cleans the gold surface through gold oxide formation (oxidation peak at 1220 mV) and removal (reduction peak at 934 mV), but also surprisingly passivates the silicon backside of the gold-coated microcantilever. Indeed, it is found that, if this step is omitted prior to PPy electropolymerization, the conjugated polymer gets electrodeposited on both side of the microcantilever. In such a case, an interpretation of the sensor's response becomes extremely difficult, if not impossible, because competing surface stress changes are generated on both sides of the microcantilever.

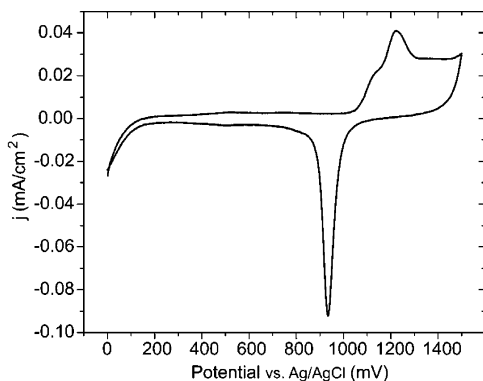


**Figure 2.** Cyclic voltammogram, recorded at a scan rate of 20 mV/s for a gold-coated microcantilever in 0.1 M HClO<sub>4</sub> solution. The Au oxide formed at potential above 1100 mV is stripped off on the cathodic sweep (sharp peak at 934 mV).

From the value of the oxide stripping charge,<sup>17</sup> we can determine the relative roughness of the gold surface. A rougher surface enhances the adhesion (mechanical interlocking) between the polymer and the gold film.<sup>18</sup> In the present case, this stripping charge did not significantly change between gold surfaces used in different experiments, indicating that the adhesion between the PPy film and the gold surface remained very similar in all of our experiments. Additional information can be extracted from the CV measurements. The shape of the oxidation peak can be indicative of the crystallographic texture of the gold film. The presence of a relatively sharp oxidation peak at 1220 mV indicates a {111} textured gold.<sup>19</sup> We have corroborated this with X-ray scattering results, which show a predominance of a polycrystalline Au(111) surface.

**2.5. Deposition of PPy.** Following the gold surface cleaning procedure, the PPy film is electropolymerized from an aqueous solution containing 0.1 M Py and 0.1 M NaDBS at a constant potential of +550 mV (vs Ag/AgCl). This value of the potential is chosen to ensure a more uniform film thickness.<sup>5</sup> The PPy film thickness can be estimated from the charge associated with the electropolymerization. For our system, we empirically found a constant of proportionality between the PPy film thickness (measured by AFM) and the charge consumed.<sup>13</sup>

$$t \text{ (nm)} = 2.8Q \text{ (mC} \cdot \text{cm}^{-2}) \quad (3)$$

Different charge–thickness relationships have been used by various groups, from experimentally determined constants to more sophisticated equations involving the film density and the molecular weight of the film and of the dopant (in proportion to the doping degree).<sup>20</sup> Because of the variability associated with these parameters, it is difficult to compare the value we have found with previously reported relations. Therefore, to obtain an accurate film thickness, the charge–thickness relationship should be calibrated for individual systems.

Figure 3 shows polymerization current simultaneously with microcantilever deflection during the electrodeposition of PPy onto the Au-coated microcantilever surface. After a time,  $t = 200$  s, the polymer films obtained and used during this study have an average thickness of  $304 \pm 9$  nm.<sup>13</sup> The green color of the PPy(DBS) film on gold resulting from light interference matches the reported color for a 300-nm thick film.<sup>5</sup> Note that monitoring the microcantilever deflection during electrodeposition of the PPy film induces some local polymerization initiated by photoexcitation on the microcantilever Si backside. This is later observed with an optical microscope and can be seen on a slight kink in both the current and the deflection data

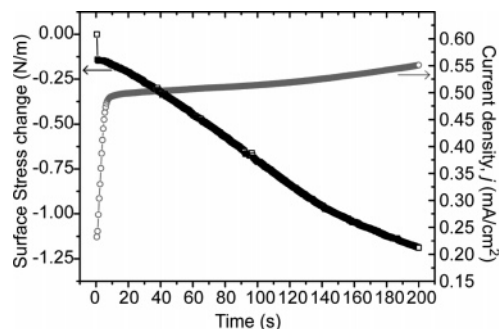


**Figure 3.** Simultaneous polymerization current (grey circle) and surface stress (black square) during PPy electropolymerization at constant potential,  $E = 550$  mV, for  $t = 200$  s.

at about 140 s. Therefore, the study of the PPy actuation properties is performed on PPy-coated microcantilevers for which the deposition-induced deflection was not monitored. The PPy(DBS) films were smooth and uniform in color when observed under an optical microscope. An AFM image of the film morphology revealed the presence of nodules ( $\sim 100$  nm in diameter), which are characteristic for such thin films.<sup>21</sup>

### 3. Results and Discussion

**3.1. Actuation of Conducting Polymers.** The reversible oxidation and reduction of a conducting polymer film can be associated with a considerable volume change of the polymer.<sup>22</sup> It has been proposed that mechanisms of actuation in conducting polymers can be divided into two contributions.<sup>23</sup> First, an intrinsic part originates from changes in conformation and in carbon–carbon bond lengths of the polymer, induced by changes in the charge density in the polymer backbone. Second, a swelling part arises from the insertion of ions from the electrolyte solution to maintain electroneutrality in the polymer film. The latter part is composed of an osmotic expansion due to insertion of ions, and their solvation shells (e.g., water molecules) inside the polymer matrix, changing the ionic concentration in the polymer and creating an osmotic pressure difference between the polymer and the electrolyte solution. This increase in osmotic pressure forces additional water molecules to enter the polymer phase and thus produces an additional increase in polymer volume.

**3.1.1. Surface Stress during Redox Reaction in PPy(DBS).** Mechanical changes in the PPy film are actuated by cyclic voltammetry in a 0.1 M NaDBS while monitoring the microcantilever deflection. The electrode potential is initially swept from its rest potential to  $-850$  mV, and back to  $+300$  mV, at a scan rate of 100 mV/s. Within this potential window, the PPy film is cycled between its oxidized and reduced states, as shown in eq 1 and Figure 1.

The reduced state is characterized by a change in charge of the polymer backbone (neutral) and a swelling of the polymer matrix, causing a bending of the microcantilever beam. Figure 4 shows the current and surface stress changes for a PPy-coated microcantilever during two oxidation/reduction cycles. Maximum microcantilever deflections are achieved when going between the anodic (oxidation) and the cathodic (reduction) peak potentials, so that most of the bending is achieved within a 400-mV potential window. The correlation between the surface stress change and the redox potentials of the polymer film is in accordance with the mass changes observed by Bay et al.<sup>24</sup> A surface stress change of  $-2.0 \pm 0.2$  N/m is obtained between these two states for the PPy(DBS) films in 0.1M NaDBS under the specific conditions used here.



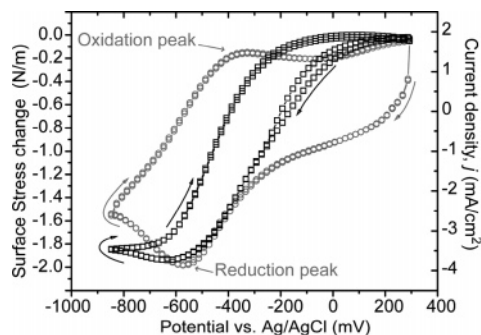


**Figure 4.** (a) Surface stress (black square) and current (grey circle) vs potential measured simultaneously during two consecutive cyclic voltammetric scans in 0.1 M NaDBS solution. The potential is swept at 100 mV/s between  $-850$  and  $+300$  mV. A change in surface stress of about 2 N/m is observed when going between the anodic and the cathodic peaks.

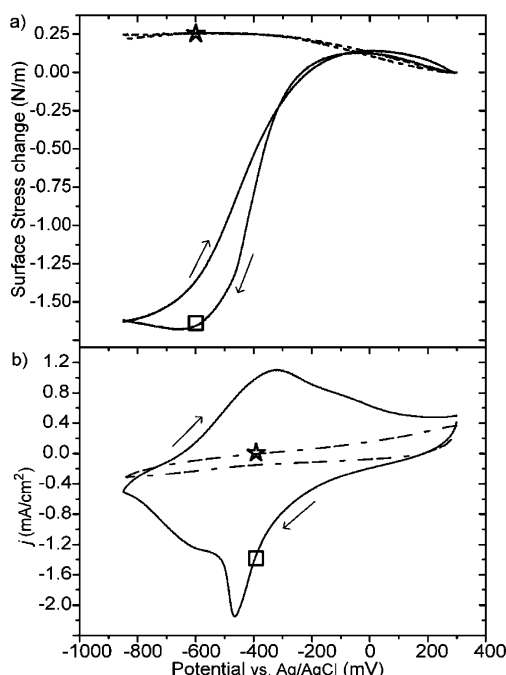


**Figure 5.** Control experiment. (a) Initially, the PPy film is actuated in 0.1 M NaCl (square), showing a compressive change in surface stress during swelling of the polymer. The same PPy(DBS) film is subsequently immersed in a redox inhibiting electrolyte, 0.1 M TBABr (star). No compressive stress is observed. (b) The CV in 0.1 M NaCl (square) shows the presence of the oxidation and reduction peaks, whereas in 0.1 M TBABr (star), the redox reaction is clearly suppressed.

**3.1.2. Redox-Inhibiting Electrolyte.** To ensure that the above-measured surface stress is indeed due to a volume change of the polymer phase, a control experiment was performed. The PPy film is actuated by cyclic voltammetry in a redox inhibiting electrolyte while monitoring the surface stress response. The microcantilever deflection signal was studied under a 0.1 M TBABr, tetrabutylammonium bromide, aqueous solution.  $\text{TBA}^+$  is a bulky cation, which will not incorporate into the polymer matrix to maintain electroneutrality in the film, hence, preventing the redox process from occurring.<sup>25,26</sup>

Figure 5a shows the surface stress response of a PPy(DBS) film during potential cycling, between  $-850$  and  $+300$  mV at a scan rate of 100 mV/s, successively in 0.1 M NaCl (square) and 0.1 M TBABr (star). At first, the film is cycled in a 0.1 M NaCl electrolyte (square), showing a typical compressive change in surface stress of about  $-1.9$  N/m, in phase with the oxidation and reduction peak potentials of the PPy(DBS) film as previ-

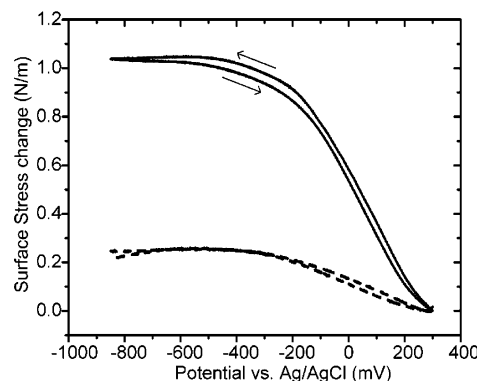


**Figure 6.** Surface stress measurement during  $\text{Br}^-$  anion adsorption (straight line) on a bare gold-coated microcantilever in 0.1 M TBABr. A change in the surface charge density of the gold surface, owing to the nature of the interaction with the anions, is responsible for the compressive change in surface stress observed when going toward positive potentials. This graph elucidates the behavior of the PPy(DBS) bending response in 0.1 M TBABr (dotted line, reproduced from Figure 5a).

ously shown in Figure 4. Subsequently, the same film is immersed in a 0.1 M TBABr electrolyte. It is now unable to undergo reduction, as shown by the disappearance of the redox peaks in the CV of Figure 5b (star). The swelling of the PPy(DBS) film is, therefore, inhibited, and the microcantilever sensor does not experience a surface stress change as shown in Figure 5a (star). From this observation, we can assert that the surface stress change measured during redox switching of PPy is indeed due to a change of volume of the conducting polymer matrix.

Nevertheless, the microcantilever is not completely motionless during potential cycling in TBABr electrolyte. For potentials below  $-200$  mV, the microcantilever can be considered static as mentioned earlier. However, above that value, it experiences a compressive change in surface stress of about  $-0.25$  N/m. This motion, which we believe is not related to the volume changes of the polymer phase, can be attributed to the interaction between the  $\text{Br}^-$  anions and the gold substrate, underneath the PPy film. Indeed, the interaction of anions with a bare gold surface results in a charge-induced surface stress, as discussed by Haiss<sup>27</sup> and Ibach.<sup>28</sup> Figure 6, shows the surface stress change of a bare gold-coated microcantilever when cycled in 0.1 M TBABr between  $-850$  and  $+300$  mV at a scan rate of 100 mV/s. A significant microcantilever deflection response is detected when a potential is applied to its surface. We observe that the surface stress curve is qualitatively similar to the one obtained for the PPy(DBS) film in TBABr. In fact, the two curves superimpose when scaled appropriately. The variation in magnitude is, therefore, attributed to the different surface areas of gold exposed in the two systems.

The paths by which the anions reach the gold-coated microcantilever substrate remain indeterminate. The underlying gold substrate may be exposed to anions, rendering the system sensitive to charge-induced surface stress through defects in the polymer matrix and/or at microcantilever edges where the PPy(DBS) film does not properly adhere to the microcantilever. Hence, in a PPy-gold-coated microcantilever structure, one should expect a competing contribution to the measured surface stress from the gold substrate if it is exposed to the electrolyte.

We note that the mechanism of the redox process is more complex when small mobile anions, such as  $\text{Br}^-$  or  $\text{Cl}^-$ , are present in the electrolyte and may be governed by both cations and anions of the supporting electrolyte.<sup>4</sup> Nevertheless, previous results of free-standing PPy(DBS) films<sup>4,24,26</sup> (i.e., no underlying

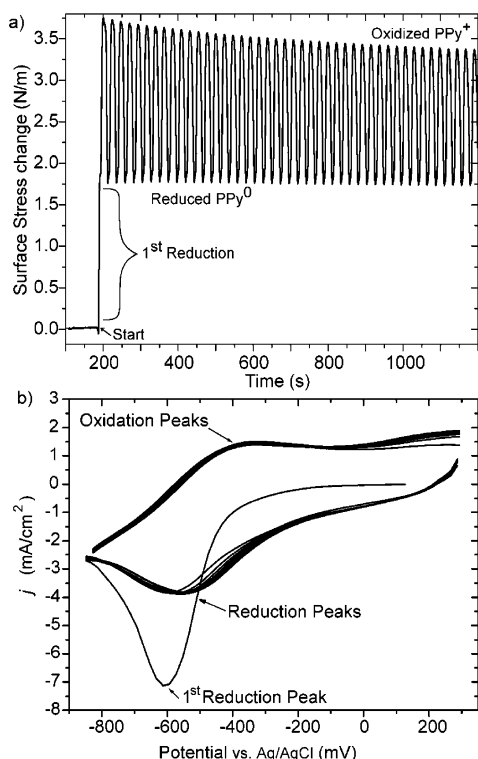


**Figure 7.** (a) PPY-coated microcantilever deflections during the first 50 cycles between  $-850$  and  $+300$  mV, in  $0.1$  M NaDBS, at a scan rate of  $100$  mV/s. The first reductive scan gives rise to a significant tensile surface stress. The following reductive scans produce a compressive change in surface stress, as expected from the swelling of the film. During multiple cycles, the peak-to-peak amplitude of the surface stress gradually decays. (b) Corresponding cyclic voltammogram showing the anomalous first reduction peak and the subsequent oxidation and reduction peaks, where the polymer is oxidized ( $\text{PPy}^+\text{DBS}^-$ ) and reduced ( $\text{PPy}^0\text{DBS}^-\text{Na}^+$ ), respectively.

gold) in small anion electrolyte indicate mainly cation motion and no apparent volume change associated with potential insertion/ejection<sup>29,30</sup> of the mobile anions. We, therefore, attribute the small compressive change in surface stress observed above  $0$  mV in Figure 5 (square) to a charge-induced surface stress, owing to anions interacting with the gold surface and not to a swelling of the  $\text{PPy}(\text{DBS})$  due to insertion of  $\text{Cl}^-$ .

**3.1.3. First Cycle.** It is interesting to examine the first reduction scan in both the CV and the surface stress data of a freshly polymerized (uncycled) PPY film. Before any electrochemical actuation takes place, the freshly prepared  $\text{PPy}^+(\text{DBS}^-)$  film is in its oxidized (doped) state. During a usual reduction process, the PPY film swells and the microcantilever experiences a compressive surface stress, i.e., bends away from the PPY-coated side. This is experimentally verified (see Figure 4) except for the very first reductive scan, where the PPY-coated microcantilever experiences a significant tensile surface stress. This discrepancy is also observable in the CV (Figure 7b) as a shift in magnitude and potential of the first reduction peak. A tensile surface stress for the first reductive scan for two independent experiments performed in different electrolyte solutions ( $0.1$  M NaDBS and  $0.1$  M NaCl) is shown in Figures 7a and 8, with a similar value of about  $+1.5$  N/m. There exists some variability in the tensile surface stress values obtained. Nonetheless, we have found an average value for 20 experiments of  $+1.0 \pm 0.5$  N/m, irrespective of the electrolyte solution. It is the first time, to our knowledge, that such an observation has been quantified. In fact, other groups have observed little or no movement during the first reduction cycle on thicker PPY films,<sup>6,30,31</sup> which implies

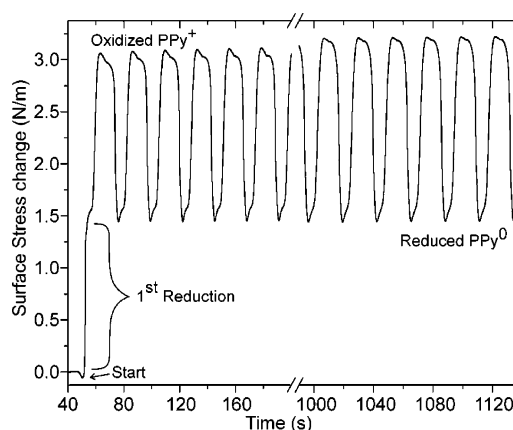


**Figure 8.** PPY(DBS)-coated microcantilever deflection during multiple cycles in  $0.1$  M NaCl at  $100$  mV/s. The first reductive scan also gives rise to a significant tensile surface stress. During multiple cycles, the peak-to-peak amplitude of the surface stress is stable over 500 cycles.

that this tensile surface stress may be a function of the film thickness. This anomalous first cathodic peak has been previously investigated, but its origins are still not completely understood. It is suggested that uncycled PPY films are irreversibly changed during the first reduction cycle. One hypothesis<sup>6</sup> is that channels are opened in the polymer matrix for the first time to allow diffusion of the cations ( $\text{Na}^+$  and its solvation shell in this case). With our observation of a tensile surface stress we envisage that the fresh  $\text{PPy}^+(\text{DBS}^-)$  film undergoes a nonreversible structural change on the microcantilever surface in which the polymer chains reorganize to accommodate the diffusion of cations. The PPY film thus shrinks and generates the observed tensile surface stress. Note that the magnitude of the tensile surface stress is comparable to the compressive surface stress observed during polymerization so that, during the first reduction cycle, the system could be relieving some of its initial stress.

**3.1.4. Multiple Cycles.** To study the lifetime of the microdevice, the long-term actuation capability of the PPY film was examined over multiple cycles. Cyclic voltammetry experiments were conducted in two different electrolyte solutions,  $0.1$  M NaDBS and  $0.1$  M NaCl, on more than 20 samples while monitoring the microcantilever deflections as a function of number of cycles.

Figure 7a shows a freshly polymerized PPY film actuated through 50 cycles from  $+300$  and  $-850$  mV (vs Ag/AgCl) at a scan rate of  $100$  mV/s in  $0.1$  M NaDBS. Figure 7b is the corresponding cyclic voltammetric data, from which we can identify the oxidation and reduction current peaks. The PPY(DBS)-coated microcantilever actuator reveals a decrease in its actuation capabilities. Indeed, the peak-to-peak surface stress amplitude, between the  $\text{PPy}^+$  and  $\text{PPy}^0$  states, decays with increasing cycle number as shown in Figure 9. This loss in actuation amplitude is quite severe and is indicative of a delamination of the polymer film, as will be discussed later.

Similar experiments were conducted in  $0.1$  M NaCl. Figure 8 shows the microcantilever deflections for a series of actuation between  $+300$  and  $-850$  mV at a scan rate of  $100$  mV/s. In this case, the peak-to-peak surface stress amplitude does not gradually decay, but rather slightly increases before stabilizing. The film reaches a value of about  $1.9$  N/m, which is relatively stable over more than 500 actuation cycles. This value is comparable in magnitude with the initial surface stress observed in NaDBS electrolyte. However, for this microcantilever-based actuator system, there is an obvious difference in the long-term

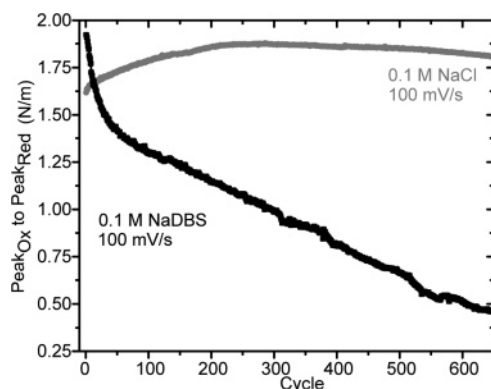


**Figure 9.** Surface stress peak-to-peak amplitude between the oxidized and reduced state of the polymer taken from the data of Figures 7 and 8. In black, the PPy(DBS) film in 0.1 M NaDBS shows a gradual loss in amplitude. In gray, the PPy(DBS) film in 0.1 M NaCl shows a slight increase and stabilization of the actuation amplitude.

actuation capabilities of PPy(DBS) films cycled either in NaDBS or NaCl electrolytes, as shown by Figure 9.

To examine in more depth the impact of the nature of the electrolyte on the long-term actuation capabilities of the PPy(DBS) film, additional experiments were conducted in another surfactant (0.1 M NaDS, sodium dodecyl sulfate) and halide (0.1 M LiCl) based electrolyte. Cycling the film in NaDS revealed a similar loss in actuation amplitude as in the NaDBS case. However, contrary to the results obtained in surfactant-based electrolytes, the actuation amplitude of the PPy(DBS) film cycled in LiCl displayed no sign of instant decline. Consequently, the surfactant property of the electrolyte is likely responsible for the degradation and loss in actuation amplitude of the polymer film. It is well established in the literature that, for a PPy(DBS) film in 0.1 M NaDBS, only the  $\text{Na}^+$  ions and their hydration shells participate in the redox process of the polymer.<sup>6</sup> The bulky  $\text{DBS}^-$  ions within the polymer are trapped and cannot diffuse in or out of the polymer matrix. Similarly, the  $\text{DBS}^-$  ions of the NaDBS-supporting electrolyte cannot enter the PPy(DBS) film.<sup>30</sup> Nevertheless, their presence in the solution has a clear impact on the actuation capabilities of PPy(DBS) films. DBS anions are amphiphilic molecules that greatly reduce the surface tension of the aqueous electrolyte. We, therefore, envision that the NaDBS electrolyte, as the film continuously swells and shrinks, progressively inserts itself in between the PPy film and the gold surface. As a result, the film gradually delaminates from the microcantilever structure, generating the observed weaker actuation. This delamination effect can be seen in Figure 10, where the evolution of the PPy-coated microcantilever actuator responses, under multiple cycles in 0.1 M NaDBS, is presented.

Figure 10 shows the PPy film actuation for increasing number of cycles. Figure 10 (square) represents a PPy film within the first 100 cycles, Figure 10 (circle) is after 500 cycles, Figure 10 (triangle), after 800 cycles, and figure 10 (star), for more than a thousand cycles. We can observe from these graphs that not only does the amplitude of actuation decreases with increasing cycling, but also the qualitative nature of the deflection data evolves. Indeed, after only a few hundred cycles, the maximum surface stress signal is no longer in phase with the oxidation and reduction current peaks. As the PPy film starts to delaminate with repeated cycling, a greater gold surface area comes in contact with the electrolyte. The interaction between the electrolyte and the gold surface begins to be more noticeable and eventually dominates. Ultimately excessive cycling results in a complete delamination of the PPy film from the micro-

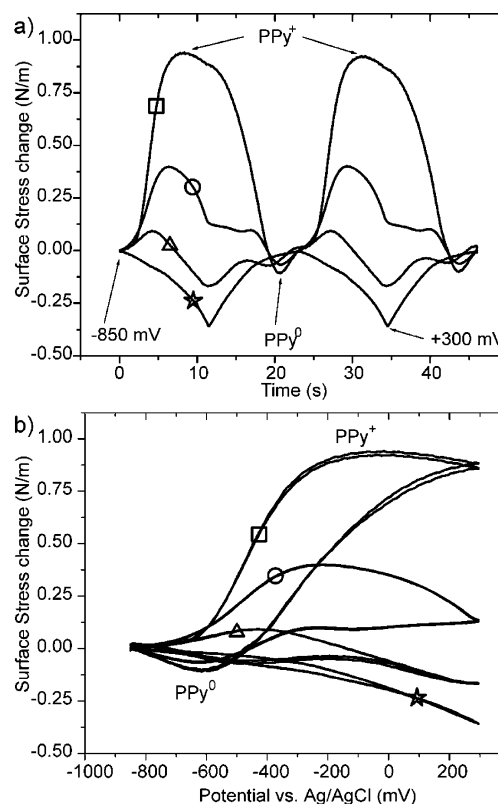


**Figure 10.** Microcantilever deflection in 0.1 M NaDBS at 100 mV/s. (a) Bending response of the PPy-coated microcantilever actuator for a polymer film cycled 100 times (square), after 500 cycles (circle), after 800 cycles (triangle), and for more than a 1000 cycles (star). Ultimately, the PPy film is completely delaminated from the gold-coated microcantilever. (b) Bending response as a function of potential. The square, circle, triangle, and star labels represent the same data as in (a). As we are only measuring a change in surface stress, the zero of the y-axis was arbitrarily chosen at  $-850$  mV.

cantilever. When the charge-induced surface stress generated by a bare gold-coated microcantilever is subtracted from the degraded response of the PPy-coated microcantilever of Figure 10 (circle), we obtain the original bending response of a fresh PPy-coated microcantilever actuator, as shown in Figure 11. Hence, an extensive cycling of a PPy(DBS) film in 0.1 M NaDBS gradually delaminates the PPy film from the microcantilever, exposing the underlying gold substrate to the electrolyte.

To determine the contribution of this competing surface stress generated by the gold substrate to the loss in actuation, we have subjected the PPy(DBS) film to a narrowed potential window. As we have previously shown, in the potential window where the polymer is in its oxidized state, any gold surface exposed generates an opposing surface stress owing to its interaction with anions. To take away this effect, we have, therefore, performed cyclic voltammetry from  $-850$  to  $-200$  mV in 0.1 M NaDBS at a scan rate of 100 mV/s on freshly polymerized PPy(DBS) films. Nevertheless, PPy(DBS) films, despite exhibiting a slower decay rate, showed a similar immediate loss in actuation amplitude. This establishes that anion interaction with the gold substrate is not the driving force of this instant shortfall in actuation in NaDBS electrolyte, but only a consequence of the delamination.

To improve the lifetime of the PPy(DBS) microactuator, the adhesion of the polymer film with the metal substrate needs to be enhanced. Several approaches are being considered, such as chemically attaching the PPy film to the gold surface via thiol-



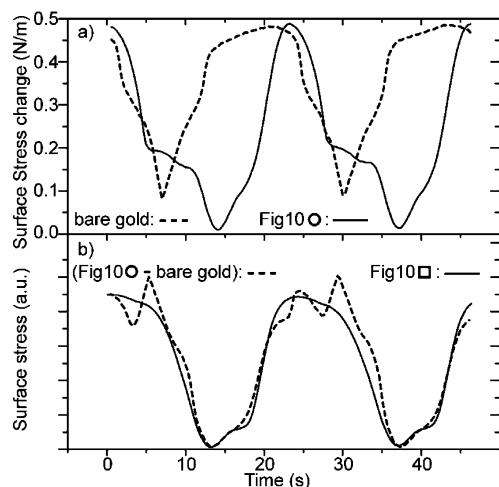


**Figure 11.** (a) The surface stress induced on a bare gold-coated microcantilever (dotted line) in 0.1 M NaDBS is superimposed with the degraded bending response of a PPy(DBS) film cycled 500 times (full line, taken from Figure 10 (circle)). (b) Bending response from a fresh PPy(DBS) film (full line, taken from Figure 10 (square)) superimposed with the differential signal of a degraded PPy(DBS) film and a bare gold-coated microcantilever in 0.1 M NaDBS. The overlap is striking, so that the degraded signal is a combination of fresh PPy(DBS) film actuation and charge-induced surface stress, owing to the interaction of the electrolyte and the gold substrate.

modified pyrrole units,<sup>32</sup> more adapted electrochemical switching techniques,<sup>33</sup> and electrolyte solutions, as well as roughening the gold to increase the mechanical interlocking.<sup>18,34</sup> We note, however, that a rougher surface will render the device more sensitive to charge-induced surface stress in the metal.<sup>35</sup>

#### 4. Conclusion

We have constructed a microactuator device by electrodepositing a PPy(DBS) film onto the gold-coated side of an AFM microcantilever. We have demonstrated that the volume change of the PPy(DBS) film with respect to the gold-coated microcantilever is responsible for the mechanical motion observed. We have measured a compressive change in surface stress of about 2 N/m when the conducting polymer is electrochemically switched between its oxidized (PPy<sup>+</sup>) and neutral (PPy<sup>0</sup>) state by cyclic voltammetry. Interestingly, we have observed the presence of a substantial tensile surface stress during the first anomalous cathodic scan, which was attributed to nonreversible structural change of the freshly polymerized PPy film. The lifetime of the microactuator device was examined in both 0.1 M NaDBS and 0.1 M NaCl electrolyte. The surfactant nature of the electrolyte (DBS molecules) was found to be likely responsible for the degradation and delamination process of the PPy film. Most importantly, we have identified two main competing origins of surface stress acting on the PPy(DBS)/gold-coated microcantilever. For the most part, a purely mechanical source, because of the volume change of the PPy(DBS) polymer with respect to the gold-coated microcantilever, strains the gold surface. Additionally, there is a charge-induced surface stress from the interaction of anions with gold exposed to the electrolyte. These findings should be considered in the design and performance optimization of future conducting polymer-covered microcantilever-based actuator devices.

**Acknowledgment.** This work was supported by the Natural Science and Engineering Research Council of Canada (NSERC). Both V.T.-C. and M.G. acknowledge the financial support given by McGill University through its McGill Major Fellowships program. M.G. thanks Le Fonds Québécois de la Recherche sur la Nature et les Technologies (FQRNT) for financial support (Doctoral Fellowship). We thank L. Y. Beaulieu and Antonella Badia for many helpful discussions and Eddie Del Campo for machining the instrument.

#### References and Notes

- (1) Smela, E. *Adv. Mater.* **2003**, *15*, 481–494.
- (2) Jager, E. W. H.; Smela, E.; Inganäs, O. *Science* **2000**, *290*, 1540–1545.
- (3) Baughman, R. H. *Synth. Met.* **1996**, *78*, 339–353.
- (4) Gandhi, M. R.; Murray, P.; Spinks, G. M.; Wallace, G. G. *Synth. Met.* **1995**, *73*, 247–256.
- (5) Smela, E. *J. Micromech. Microeng.* **1999**, *9*, 1–18.
- (6) Pei, Q.; Inganäs, O. *J. Phys. Chem.* **1993**, *97*, 6034–6041.
- (7) Jager, E. W. H.; Inganäs, O.; Lundström, I. *Science* **2000**, *288*, 2335–2338.
- (8) Bar-Cohen, Y.; Sherit, S.; Lih, S.-S. *Smart Materials and Structures. Proc. SPIE-Int. Soc. Opt. Eng.* **2001**, *4329*, 319–327.
- (9) Lahav, M.; Durkan, C.; Gabai, R.; Katz, E.; Willner, I.; Welland, M. E. *Angew. Chem., Int. Ed.* **2001**, *40*, 4095–4097.
- (10) Roemer, M.; Kurzenknabe, T.; Oesterschulze, E.; Nicoloso, N. *Anal. Bioanal. Chem.* **2002**, *373*, 754–757.
- (11) Lang, H. P.; Hegner, M.; Gerber, Ch. *Nanotechnology* **2002**, *13*, R29–R36.
- (12) Godin, M.; Williams, P. J.; Tabard-Cossa, V.; Laroche, O.; Beaulieu, L. Y.; Lennox, R. B.; Grütter, P. *Langmuir* **2004**, *20*, 7090–7096.
- (13) Tabard-Cossa, V.; Godin, M.; Beaulieu, L. Y.; Grütter, P. *Sens. Actuators, B* **2005**, *107*, 233–241.
- (14) Godin, M.; Laroche, O.; Tabard-Cossa, V.; Beaulieu, L. Y.; Williams, P. J.; Grütter, P. *Rev. Sci. Instrum.* **2003**, *74*, 4902–4907.
- (15) Godin, M.; Tabard-Cossa, V.; Williams, P. J.; Grütter, P. *Appl. Phys. Lett.* **2001**, *79*, 551–553.
- (16) Lipkowsky, J.; Schmickler, W.; Kolb, D. M.; Parsons, R. *J. Electroanal. Chem.* **1998**, *452*, 193–197.
- (17) This value is obtained by integrating the area under the cathodic peak.
- (18) Pyo, M.; Bohn, C. C.; Smela, E.; Reynolds, J. R.; Brennan, A. B. *Chem. Mater.* **2003**, *15*, 916–922.
- (19) Golan, Y.; Margulis, L.; Rubinstein, I. *Surf. Sci.* **1992**, *264*, 312–326.
- (20) Pei, Q. G.; Qian, R. *Electrochim. Acta* **1992**, *37*, 1075–1081.
- (21) Smela, E.; Gadegaard, N. *J. Phys. Chem. B* **2001**, *105*, 9395–9405.
- (22) Smela, E.; Gadegaard, N. *Adv. Mater.* **1999**, *11*, 953–957.
- (23) Bay, L.; Jacobsen, T.; Skaarup, S.; West, K. *J. Phys. Chem. B* **2001**, *105*, 8492–8497.
- (24) Bay, L.; Mogensen, N.; Skarup, S.; Sommer-Larsen, P.; Jorgensen, M.; West, K. *Macromolecules* **2002**, *35*, 9345–9351.
- (25) Rammelt, U.; Bischoff, S.; El-Dessouki, M.; Schulze, R.; Plieth, W.; Dunsch, L. *J. Solid State Electrochem.* **1999**, *3*, 406–411.
- (26) Takashima, W.; Pandey, S. S.; Kaneto, K. *Sens. Actuators, B* **2003**, *89*, 48–52.
- (27) Haiss, W. *Rep. Prog. Phys.* **2001**, *64*, 591–648.
- (28) Ibach, H. *Surf. Sci. Rep.* **1997**, *29*, 193–263.
- (29) Skaarup, S.; West, K.; Gunaratne, L. M. W. K.; Vidanapathirana, K. P.; Careem, M. A. *Solid State Ionics* **2000**, *136–137*, 577–582.
- (30) Shimoda, S.; Smela, E. *Electrochim. Acta* **1998**, *44*, 219–238.
- (31) Maw, S.; Smela, E.; Yoshida, K.; Sommer-Larsen, P.; Stein, R. B. *Sens. Actuators, A* **2001**, *89*, 175–184.
- (32) Willicut, R. J.; McCarley, R. L. *Langmuir* **1995**, *11*, 296–301.
- (33) Spinks, G. M.; Xi, B.; Zhou, D.; Truong, V.-T.; Wallace, G. G. *Synth. Met.* **2004**, *140*, 273–280.
- (34) Idla, K.; Inganäs, O.; Standberg, M. *Electrochim. Acta* **2000**, *45*, 2121–2130.
- (35) Weissmüller, J.; Viswanath, R. N.; Kramer, D.; Zimmer, P.; Würschum, R.; Gleiter, H. *Science* **2003**, *300*, 312–315.